Endothelial damage induced by Shiga toxins delivered by neutrophils during transmigration

JLB

Article

Endothelial damage induced by Shiga toxins delivered by neutrophils during transmigration

Maurizio Brigotti,[*,1] Pier Luigi Tazzari,[†] Elisa Ravanelli,[*] Domenica Carnicelli,[*] Stefania Barbieri,[*] Laura Rocchi,[*] Valentina Arfilli,[*] Gaia Scavia,[‡] Francesca Ricci,[†] Andrea Bontadini,[†] Roberta R. Alfieri,[§] Pier Giorgio Petronini,[§] Carmine Pecoraro,[||] Alberto E. Tozzi,[¶] and Alfredo Caprioli[‡]*

[*]Dipartimento di Patologia Sperimentale, Università di Bologna, Italy; [†]Servizio di Immunoematologia e Trasfusionale, Ospedale S. Orsola-Malpighi, Bologna, Italy; [‡]Istituto Superiore di Sanità, Rome, Italy; [§]Dipartimento di Medicina Sperimentale, Sezione di Patologia Molecolare e Immunologia, Università di Parma, Parma, Italy; [||]Ospedale Santobono, Naples, Italy; and [¶]Ospedale Pediatrico Bambino Gesù, Rome, Italy

RECEIVED JULY 15, 2009; REVISED MARCH 11, 2010; ACCEPTED MARCH 17, 2010. DOI: 10.1189/jlb.0709475

ABSTRACT

The endothelial damage induced by Stx represents the main pathogenic event in the HUS associated with STEC infections in humans. Stx, released in the gut by bacteria, enter the bloodstream and are targeted to renal endothelia. The role of PMN as a toxin carrier has been the object of controversy. In this paper, we confirm the binding of Stx1 to PMN, also showing its degranulating effects on full-loaded leukocytes, and support the carrier role of PMN by using a two-chamber transmigration device, in which PMN, loaded in vitro with different amounts of Stx1, transmigrated through confluent monolayers of endothelial cells, mimicking the toxin-induced renal endothelial injury. Stx1 was transferred during PMN transmigration, impairing protein synthesis and triggering production of proinflammatory cytokines in endothelial cells. PMN, carrying low toxin amounts, induced the release of high levels of cytokines in viable endothelial cells, whereas cytokine production was blocked in cells challenged with PMN fully loaded with Stx as a result of an almost total impairment of translation and of the activation of the apoptotic program. In agreement with previous unexplained observations in animal models, the results obtained with our experimental setting suggest that a self-amplifying circle triggered by low doses of toxin may lead to the production of proinflammatory mediators of renal damage in HUS. *J. Leukoc. Biol.* 88: 201–210; 2010.

Introduction

STECs are food-borne pathogens causing severe illnesses in humans, such as the HUS, the most common cause of acute renal failure in early childhood [1–4].

The main steps in the pathogenesis of STEC-associated HUS include the colonization of the gut by STEC, the release of Stx in the intestinal lumen, their absorption into the blood circulation, and their delivery to the renal and cerebral endothelia endowed with specific toxin receptors [5–7]. It is now generally accepted that the main virulence factor of STEC is Stx and that the renal endothelial injury induced by the toxins is the primary pathogenetic event in HUS [6]. STEC may produce two main types of toxins, Stx1 and Stx2, which are composed of a catalytic A chain noncovalently linked to a pentamer of B subunits that mediates the binding to glycolipid receptors (usually Gb3), present on the surface of target cells [7]. The effects of Stx on target cells are related to their enzymatic action, consisting of the removal of a specific adenine base from 28S rRNA in ribosomes [8] and of the abstraction of multiple adenines from DNA in the nucleus [9, 10]. Despite this knowledge, the consequences of the molecular damages to ribosomes and DNA induced by Stx within target cells are not simple to predict. On one hand, the Stx challenge induces apoptotic cell death [10, 11], occurring after 24–36 h of treatment in a dose-related manner [12]. On the other hand, a specific cellular response not related to apoptosis has been largely described. In particular, the treatment of endothelial cells with both Stx leads to the increased mRNA levels and protein expression of a small number of human genes, in particular, 25 genes by Stx1 and 24 by Stx2 [13]. Most of these genes encode proteins associated with inflammatory responses, such as IL-8 and MCP-1 [13, 14]. It is believed that such response patterns might contribute to HUS pathogenesis through the recruitment of inflammatory cells in the kidney [5, 6].

Abbreviations: Gb3=globotriaosylceramide, HUS=hemolytic uremic syndrome, MCV=mean channel value of fluorescence, STEC=Shiga toxin-producing *Escherichia coli*, Stx=Shiga toxin(s)

1. Correspondence: Dipartimento di Patologia Sperimentale, Università di Bologna, Via San Giacomo, 14, Bologna, Italy 40126. E-mail: maurizio.brigotti@unibo.it

Some issues that still need to be clarified in the pathogenesis of HUS are the entry of the toxins into the circulation and their delivery to renal endothelial cells. As for the latter, free Stx have never been found in the serum of patients with HUS [3, 15]. Conversely, Stx have been detected by specific antibodies on the surface of circulating PMN of HUS patients, thus suggesting a role of these blood cells as a toxin carrier [16, 17]. Although recent papers have questioned these findings [18, 19] by reporting the lack of specific binding of Stx to PMN, other studies have confirmed the presence of Stx on PMN from HUS patients [20, 21], exploiting this feature for the diagnosis of STEC infection. More recently, the binding of Stx1 and Stx2 to PMN in human blood has been demonstrated by Griener et al. [22] using immunofluorescence and by our group [23] using direct and indirect flow cytometric analysis and binding experiments with radiolabeled toxins. In particular, we also showed that Stx bind to the surface of human mature PMN but not to immature PMN from G-CSF-treated donors and confirmed this result using the human myeloid leukemia cell (HL-60) model for inducible granulocytic differentiation [23]. Further evidence of such a binding is the delay of the spontaneous apoptosis observed in PMN carrying Stx [23], also observed in PMN from HUS patients [24].

In the present study, we confirm further that Stx bind to PMN and present a comprehensive experimental model to investigate the mechanism of toxin transfer from PMN to endothelial cells and the response of these cells to intoxication. We investigated specifically the binding of Stx to PMN, the degranulating effect induced by Stx, the transmigration of Stx-positive PMN, the passage of the toxic ligand to the endothelial cells, and the effects of such a passage on protein synthesis, on cell viability, and on the release of inflammatory cytokines involved in HUS pathogenesis.

MATERIALS AND METHODS

Toxins

Stx1 was purified according to a method described previously [25]. Stx1 preparation contained low amounts of bacterial LPS (2–3 ng/mg), as assayed by using the *Limulus* amoebocyte lysate Pyrogent® plus (Cambrex, Walkersville, MD, USA). Iodination of Stx1 (100 μg) was performed with two Iodo beads (Pierce, Rockford, IL, USA) and 500 μCi Na^{125}I (2.125 Ci/μ atom, 100 mCi/ml; Amersham Pharmacia Biotech, Bucks, UK), according to the manufacturer's instruction. The biological activity of the radiolabeled toxin was assessed by testing the binding to immobilized Gb3 (globotriose-Fractogel, IsoSep AB, Lund, Sweden) and by comparing the IC_{50} of radiolabeled and native toxins on HUVEC translation.

Cell cultures and protein synthesis

HUVEC were cultured and checked for the expression of the von Willebrand factor as described previously [10, 26]. Protein synthesis was measured as the rate of incorporation of labeled leucine during a 30-min incubation of the cell monolayers in the complete medium containing 0.4 mM leucine and trace amounts of [^{3}H]leucine. This procedure has been described in detail elsewhere [27]. HUVEC were challenged, as indicated in the legends to figures or in the table, with PMN carrying Stx.

Binding of native or radiolabeled Stx1 to PMN

Highly purified PMN (98% lobulated nuclei) were isolated under endotoxin-free conditions from buffy coats of three different healthy donors after centrifugation over Ficoll Paque, followed by dextran sedimentation and hypotonic lysis of contaminating erythrocytes, as described previously [23, 28]. For binding experiments, Eppendorf tubes were precoated with PBS containing 1% BSA to avoid nonspecific loss of toxins [29]. PMN (2×10^6/ml) were incubated with different concentrations of unlabeled or labeled Stx (0.5–150 nM) for 90 min at 37°C in the same buffer. The cells were spun down at 200 g for 5 min and washed three times with 0.6 vol of the same buffer at 37°C. The extent of binding of native Stx to PMN was measured by flow cytometry as described below, whereas the binding of [^{125}I]Stx1 was quantified by counting the cell-associated radioactivity with a γ-counter. The binding of radiolabeled Stx1 in the presence of a 50-fold excess of native, unlabeled Stx1 (nonspecific binding) was subtracted in each experiment. Alternatively, PMN carrying Stx on their membrane were used immediately in the transmigration assay described below. In this case, they were finally resuspended in RPMI containing 2.5% FCS at 37°C.

Detection of Stx1 bound to PMN

Stx1 bound on PMN was detected by flow cytometry as described previously [20]. PMN carrying Stx1 (see above) were incubated with a mouse mAb against Stx1 in the presence of human serum to saturate FcRs on PMN. After incubation with FITC-goat anti-mouse IgG, flow cytometric analysis was used to reveal the PMN-bound fluorescence. Cells were visualized by a cytogram that combined forward-scatter versus 90° side-scatter, and fluorescence was analyzed by a cytogram that combined 90° side-scatter and fluorescence and by a single-fluorescence histogram. PMN were checked by staining with mAb to antigens associated to granulocytes (FITC-CD16 and FITC-CD65, Beckman Coulter, Miami FL, USA). The MCV of the single-fluorescence histogram was chosen as an objective parameter to measure the extent of binding of Stx to PMN [20]. The single values were calculated by subtracting the control MCV (range 0.4–0.6), i.e., the MCV of PMN from the same donor incubated with primary and secondary antibodies in the absence of the toxin. The same values (MCV=0.4–0.6) were obtained if anti-Stx1 mouse mAb were omitted in the assay in the presence of toxins and secondary antibodies. The assay has been validated previously by comparing control subjects and HUS patients in a blinded manner [20] and by challenging Stx-positive PMN with a negative control antibody [21].

PMN degranulation assays

PMN were incubated as described above with Stx1 (see Fig. 3). After 90 min at 37°C, the occurrence of degranulation was revealed by assessing the presence of the specific degranulation markers (CD11b, CD66b, CD63) on PMN surface by flow cytometry. Samples were treated with a fixative solution (VitaLyse, BioE, St. Paul, MN, USA), and after two washings with PBS, 3×10^5 cells were pelleted and incubated for 20 min at room temperature with the following mAb: PE-CD63 (Beckman Coulter), allophycocyanin-CD11b (Becton Dickinson, Franklin Lakes, NJ, USA), or unconjugated CD66b (Becton Dickinson). In the latter case, after two further washings with PBS, cells were incubated with FITC anti-mouse IgG (Beckman Coulter). Controls were run with an appropriate IgG isotype. Samples were evaluated by flow cytometry (FC500 cytometer, equipped with two lasers, Beckman Coulter), and histograms were obtained by the CXP-dedicated program (Beckman Coulter).

Transmigration assay

HUVEC (2.5×10^5) were seeded in the upper chamber of Transwell (12 mm diameter, 3 μm pore size, Costar, Cambridge, MA, USA), precoated with fibronectin (50 μg/ml for 30 min), and the cells were grown at 37°C in 5% CO_2-supplemented air for 2 days to obtain a confluent monolayer. PMN were added at 1×10^6 cells/well to the top chamber containing RPMI with 2.5% FCS. The chemoattractant IL-8 (5 nM) was added to the same medium present in the lower chamber. After 2 h at 37°C, the PMN that had transmigrated into the lower chamber were collected, washed with PBS, and pelleted as described above. Proteins present in the pellet and in the lower chamber were precipitated with 10% TCA, resuspended in KOH 0.5 N, and quantified by the Bio-Rad protein assay (Bio-Rad, Hercules, CA,

USA) [30] with BSA as standard. In each experiment a standard curve (number of cells/protein content) was constructed with known amounts of PMN ($0.25–1\times10^6$), washed, pelleted, and TCA-precipitated as described above. The number of transmigrated PMN was determined by plotting the values of protein determinations on the standard curve. The coefficient of determination was, in all cases, >0.98. The protein content of 1×10^6 PMN was ~40 μg. Nontransmigrated PMN present in the top chamber were removed, and the HUVEC monolayer was washed gently three times with 250 μl PBS to detach adherent leukocytes. Finally, the number of PMN present in the combined culture medium and washings was determined as described above. Total recovery percent (% PMN in the upper chamber+% PMN in the lower chamber) after the transmigration assay was 89.3 ± 10.7% (mean±SD; n=6). To determine the protein synthesis rate in HUVEC challenged with transmigrating PMN, the upper chamber was removed gently, and its edges were cut carefully with a scalpel so that the bottom microporous membrane containing the endothelial monolayer could be transferred to new culture plates. Fresh medium for the HUVEC culture [10, 26] was added, and after 16 h, the translation rate was measured as described above. The overnight culture supernatants were collected for cytokine determinations.

Detection of chemokines by ELISA

IL-8 and MCP-1 proteins present in culture supernatants from control, toxin-treated HUVEC and HUVEC challenged with PMN carrying Stx were quantified by enzyme immunoassay using standards ranging from 31.25 to 2000 pg/ml, according to the manufacturer's instructions (quantikine human IL-8 and human MCP-1 immunoassay; R&D Systems Inc., Minneapolis, MN, USA).

Detection of apoptosis and necrosis

Cell apoptosis and necrosis were assessed morphologically on HUVEC using fluorescence microscopy. After transmigration of control or Stx1-treated PMN, HUVEC were incubated overnight (see above), and then, they were detached from the microporous membrane by treatment with trypsin 0.1% for 2.5 min. Detached cells were stained with Hoechst 33342 (3 μg/ml) and propidium iodide (2.5 μg/ml) and their nuclear morphology examined by fluorescence microscopy. No significant changes in total protein contents were observed in each condition, as quantified by the Bio-Rad protein assay [30].

Data analysis

Data were stored in a Microsoft Excel file. Data analysis was performed with SPSS, Version 14.0. Differences in continuous variables were tested with t-test after controlling the normality of their distribution. Correlation between variables was assessed through calculation of the Pearson correlation coefficient.

RESULTS

A model of PMN transmigration through an endothelial cell monolayer was deployed by using a two-chamber transmigration device in which HUVEC were seeded in the upper chamber to form a confluent monolayer. Highly purified, endotoxin-free PMN [23, 28], isolated from different healthy donors, were treated with Stx1 to obtain amounts of bound toxin comparable with those observed in the PMN from HUS patients [20, 21]. PMN were then stimulated to transmigrate through the monolayer by the presence of IL-8 in the lower chamber.

Binding of Stx1 to isolated PMN

The binding of Stx1 to PMN was performed with native and radiolabeled Stx1. In the former case, the amount of Stx1 bound to PMN was detected by indirect flow cytometric analysis by measuring the fluorescence associated to PMN and expressed as MCV [20]. The latter parameter was used in previous studies to measure the maximum Stx-binding capacity of PMN from healthy donors (MCV~3) [20, 23] and to detect Stx in the blood of patients with HUS (MCV=0.7–5) [21]. The dose-response curve of the interaction PMN-Stx1 is shown in **Figure 1A**. When Stx1 concentrations were increased progressively, starting from 0.5 nM, the measured MCV increased gradually until the maximum binding capacity was reached (Fig. 1A). Under these saturating conditions (≥50 nM Stx1), we obtained fluorescence values (highest MCV values of Fig. 1, A and B) similar to the maximum values observed in previous studies in HUS patients [20, 21], as depicted in the single-histogram analysis shown in **Figure 2B**. The exact amount of toxin bound to PMN at saturation was measured with radiolabeled [^{125}I]Stx1 (50 nM) by counting the radioactivity associated to PMN after extensive washing. The value (0.33 pmol/10^6 PMN±0.04; mean±SD; n=3) was obtained after subtraction of the radioactivity measured in the presence of 50-fold excess unlabeled Stx1 (nonspecific binding). The calculated number of binding sites/PMN (201,400±13,000 mean±SD; n=3) was similar to previous reported values [17, 23]. PMN, fully loaded with [^{125}I]Stx1, were used in some of the following experiments (see below).

Stx1 does not inhibit PMN transmigration

Transmigration experiments were performed with control and Stx1-treated PMN. Figure 1B shows the relationship between the extent of Stx1 binding to PMN, expressed as MCV, and the transmigration of Stx1-treated PMN through the endothelial cell monolayer to the lower chamber after 2 h. PMN transmigration (675,000±127,000; mean±SD; n=6) was not impaired by the presence of Stx1 on the PMN membranes, even at saturating conditions (MCV~3; Fig. 1B).

Stx1 induces PMN degranulation

PMN possess different type of granules sequentially mobilized during transmigration from the bloodstream to the site of inflammatory recruitment [31–33]. The membrane luminal side of these granules is rich in specific proteins that appear on the cell surface after exocytosis, giving evidence of degranulation. Two types of granules are marked with CD11b: the secretory granules, which fuse with the PMN plasma membrane during the initial interaction with endothelium, providing a variety of membrane-bound receptors, and the gelatinase granules, which release several proteases during transmigration, allowing PMN to cut the basal membrane [31–33]. Exocytosis of these granules is not harmful for endothelium. On the contrary, the potentially dangerous content of primary granules (marked by CD63) and secondary granules (marked by CD66b and CD11b) is released in the extravascular space supporting bacterial clearance [31–33]. **Figure 3** shows a positive, dose-dependent trend in the activation and degranulation of PMN by Stx1 during the 90-min incubation necessary to bind the toxin before the transmigration assay. However, a significant increase in the expression of all degranulation markers with re-

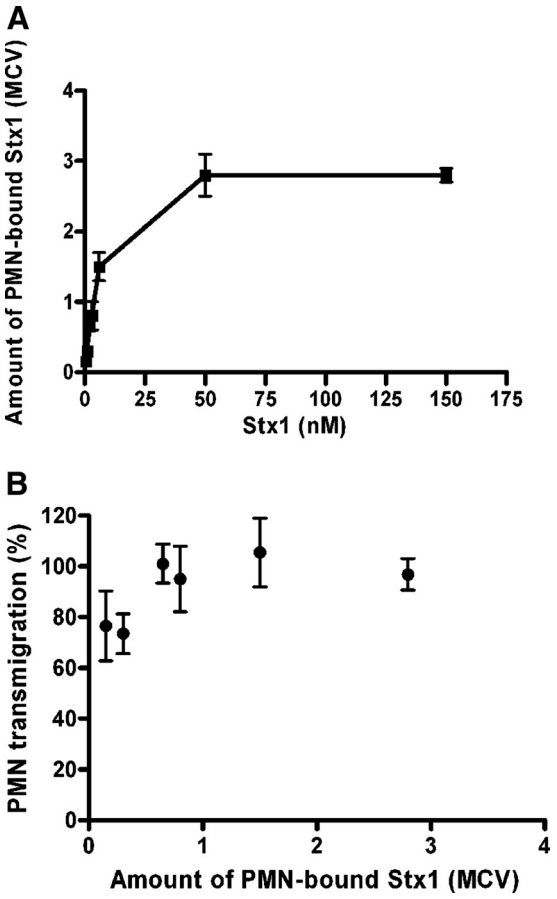

Figure 1. Binding of Stx1 to PMN and transmigration of PMN populations carrying different amounts of Stx on their membrane. (A) PMN were treated with increasing concentrations of Stx1, and the binding of the toxin to PMN was assessed by flow cytometry, as described in Materials and Methods, and expressed as MCV. The data are the means ± SD. (B) Transmigration assay is described in Materials and Methods, and the percent of transmigration of Stx1-loaded PMN with respect to control PMN is shown. The data are the means ± SD from three independent experiments. In the presence of toxin, no significant differences were observed with respect to control transmigration ($P>0.05$).

spect to basal level was observed only with PMN fully loaded with Stx1. After transmigration and consequent stimulation by IL-8, degranulation was observed at the same extent in Stx1-treated and Stx1-negative PMN, as assessed by detection of the marker CD66b (**Fig. 4**). Thus, the already degranulated toxin-treated PMN appeared hyporesponsive to a second activating stimulus. It should be noted that the potentially harmful products released by PMN did not interfere in the transmigration assay, as they were lost during the washings necessary to eliminate free, unbound toxins.

Transfer of Stx1 from PMN to endothelial cells during transmigration

Stx1 was no longer detectable on PMN after their transmigration, as indicated by the disappearance of the fluorescent staining from the cells migrated to the lower chamber (Fig.

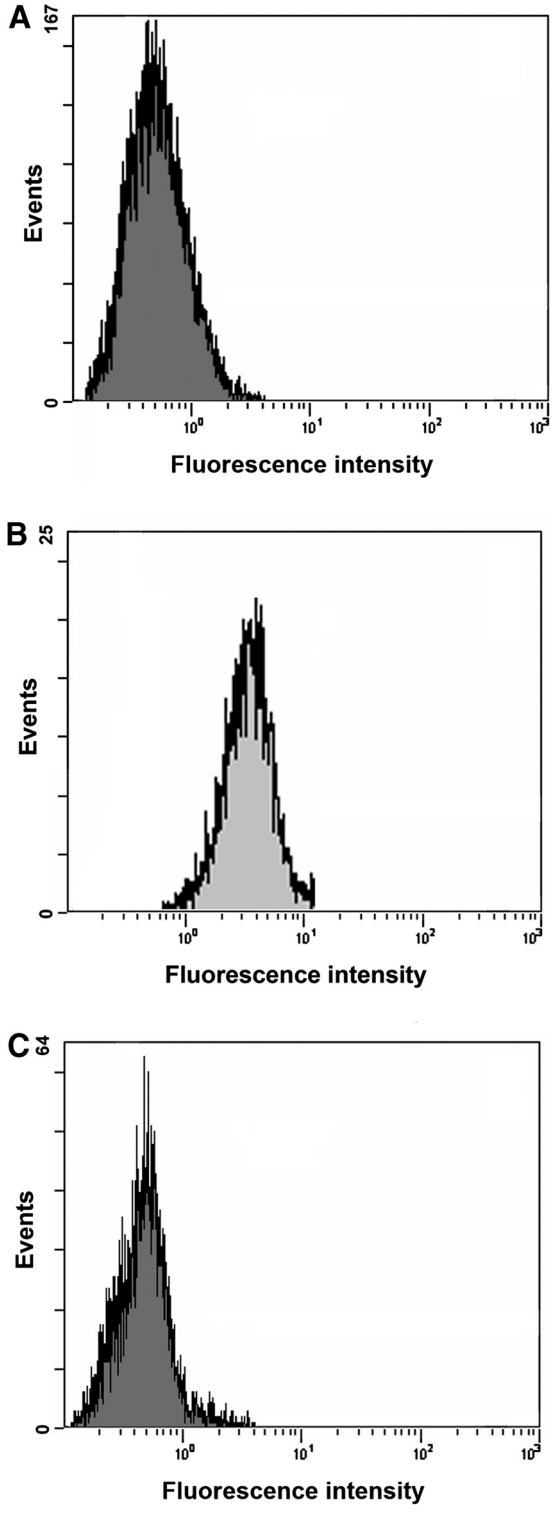

Figure 2. Cytogram profiles of flow cytometry detection of Stx on PMN membranes. PMN, isolated from healthy donors, were untreated (A); treated with 50 nM Stx1 (B); or treated with 50 nM Stx1, followed by transmigration through an endothelial cell monolayer, as described in Materials and Methods (C). The single-histogram analysis is representative of three independent experiments in which significant differences ($P<0.001$) between the fluorescence values of fully loaded PMN before (MCV=2.83±0.30) and after (MCV=0.02±0.04) transmigration were observed.

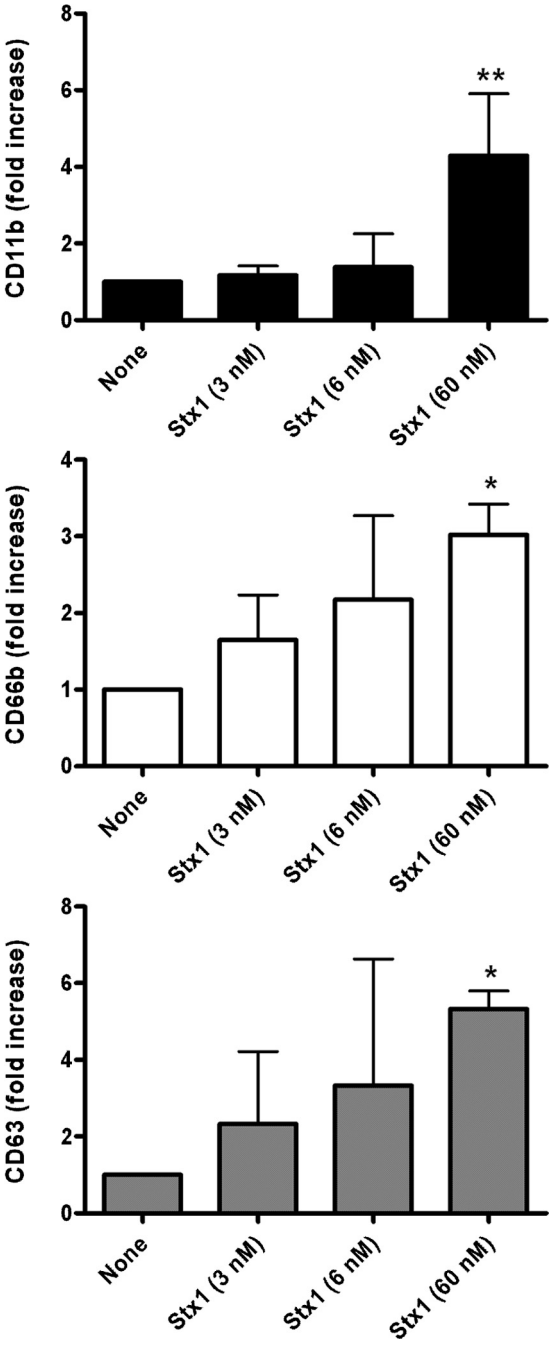

Figure 3. Degranulation of PMN treated with Stx1. PMN were treated as described in Materials and Methods with Sx1 (60 nM, 6 nM, and 3 nM), obtaining three populations having full saturation (MCV~3), half-saturation (MCV~1.5), and low saturation (MCV~0.8) of receptors, respectively. The presence on the PMN surface of CD11b (present on the membrane of secretory, gelatinase, and secondary granules), CD66b (present on the membrane of secondary granules), and CD63 (present of the membrane of primary granules), as evidence of degranulation, was assessed by direct or indirect flow cytometric analysis as described in Material and Methods. Data are means ± SD from three independent experiments. The ratios between the expression of the degranulation markers in toxin-treated cells and those in control cells give the fold increase. *, $P < 0.001$; **, $P < 0.05$.

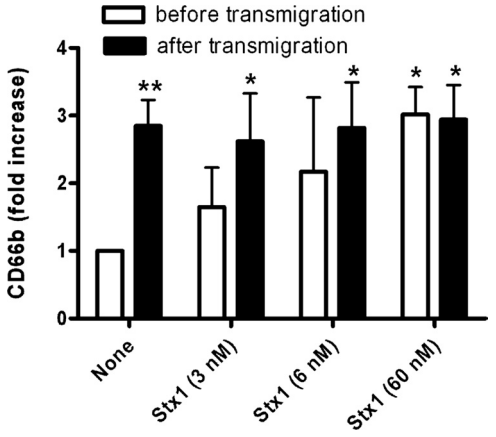

Figure 4. Degranulation of PMN after transmigrating stimuli. PMN were treated as described in the legend to Figure 3, and then they were stimulated to transmigrate through HUVEC monolayers in the presence of IL-8 (5 nM), as described in Materials and Methods. The extent of expression of CD66b was assessed in the transmigrated PMN and compared with that obtained before transmigration. Data are means ± SD from three independent experiments. The ratios between the expression of the degranulation marker CD66b in the population of PMN indicated that in the figure and those in control, nontransmigrated cells give the fold increase. *, $P < 0.05$; **, $P < 0.001$.

2C), which had MCV similar to those of the control PMN (Fig. 2A). Further evidence was obtained by treating PMN from three different donors with [^{125}I]Stx1 at saturating conditions (see above) and by comparing their specific radioactivity before and after the 2-h transmigration assay. The specific radioactivity of the PMN decreased by one order of magnitude after their transmigration to the lower chamber. Conversely, the specific activity of nonmigrated PMN remaining in the upper chamber was only slightly reduced (**Table 1**). After the passage of 60% of total PMN present in the assay, the percentage of total radioactivity associated to HUVEC was 64.5 ± 9.2, confirming the transfer of the toxic ligand to the endothelium.

Inhibition of protein synthesis in endothelial cells challenged with PMN carrying Stx1

As Stx are well known as specific inhibitors of translation which irreversibly damage ribosomes, the effect of the transmigration of PMN carrying different amounts of Stx on the protein synthesis of the endothelial cell monolayers was evaluated (**Fig. 5**). After the 2-h transmigration assay, the bottom part of the upper chamber with adherent HUVEC was transferred to new culture plates. Fresh medium was added, cells were incubated overnight, and finally, the translation rate was measured, and the overnight culture supernatants were collected for cytokine determinations (see below). The overnight incubation is sufficient to allow the internalization of the toxin, the formation of Stx-dependent intracellular injuries, and the synthesis and release of proinflammatory cytokines by HUVEC, as assessed previously with soluble Stx1 [10, 34].

HUVEC protein synthesis was found to be impaired, and the extent of inhibition was related strictly to the amount of Stx

TABLE 1. Disappearance of Radiolabeled Stx1 from PMN after Transmigration

Source of PMN	Specific radioactivity ratio[a]	
	Nonmigrated PMN	Transmigrated PMN
Donor 1	1.37	0.01
Donor 2	0.97	0.11
Donor 3	0.45	0.11
Mean ± SD[b]	0.93 ± 0.46	0.08 ± 0.06

[a]Ratio between the specific radioactivity of the indicated PMN populations and the specific radioactivity of PMN before the transmigration experiment. As described in the text, treatment of PMN with 50 nM [^{125}I]Stx1gave full saturation of the receptors, as reported in ref. [17]. [b]$P < 0.05$.

present on the migrating PMN, measured as MCV (Fig. 5). The specificity of Stx-mediated damage in endothelial cells was demonstrated by the neutralizing effect of anti-Stx1 mAb (6 μg) added in the upper chamber during the transmigration assay (data not shown). In the absence of the chemoattractant, fully loaded, nontransmigrating PMN (MCV~3) gave low inhibition of protein synthesis in HUVEC (10.1±13.2; mean±SD; n=3), probably caused by gravity-dependent endothelium-PMN interactions.

Release of proinflammatory cytokines involved in HUS pathogenesis by Stx-treated endothelial cells

It is known that the treatment of endothelial cells with Stx1 and Stx2 leads to increased mRNA levels and protein expression of chemokines, such as IL-8 and MCP-1 [13, 14], of cell adhesion molecules [35], and of several other cytokines involved in HUS pathogenesis [13]. The molecular link between cytokine expression and the enzymatic action of the Stx is the ribosome, as the specific damage of ribosomal 28S RNA induced by the toxins is indispensable and sufficient to activate stress kinase cascades, which in turn, induce the nuclear transcription of the proinflammatory genes [9, 36, 37]. However, the same ribosomal damage might interfere with the translation into proteins of the proinflammatory cytokine mRNAs [9]. Therefore, the relationship between cytokine expression and protein synthesis inhibition is not simple to predict.

The production of IL-8 was evaluated in HUVEC challenged with Stx1-positive PMN populations, having MCV representative of those observed in HUS patients. Transmigration through the endothelial cell monolayers of PMN, having MCV between the detection limit and 1.5, caused a protein synthesis inhibition between 30% and 60% (vertical dotted lines, **Fig. 6A**). This was accompanied by a significant up-regulating effect on IL-8 expression (Fig. 6B). In this case, signals deriving from ribosomal damage via stress-activated kinase cascades are present in the nucleus to indicate the need for transcription, and the resulting mRNA is translated into a protein sequence, as the protein synthesis machinery is not devoid completely of activity. By contrast, fully loaded PMN (MCV~3) induced in HUVEC a protein synthesis inhibition higher than 60%, with a significant impairment of IL-8 up-regulation, probably as messengers remained untranslated in the cytoplasm.

The same behavior was observed when the amount of the chemokine MCP-1 was measured in HUVEC culture supernatants after PMN transmigration. The trend of MCP-1 up-regulation shown in Figure 6C was similar to that of IL-8, suggesting that the relationship between cytokine expression and protein synthesis impairment induced by Stx might be a general phenomenon. Interestingly, with both chemokines, the maximal up-regulating effect was observed when HUVEC translation was ~50%, inhibited by the transmigration of Stx1-carrying PMN having ~30% saturation (MCV ~1; Fig. 6). This up-regulating effect was abrogated completely by the presence of neutralizing mAb to Stx1 (6 μg), ruling out the involvement of contaminating molecules (such as LPS) in the phenomenon (data not shown). We cannot exclude the presence of contaminating PMN trapped underneath HUVEC monolayers or in the pores and basal side of the filter, as ~10% of PMN (1×10^5 cells) was not recovered after transmigration (see Materials and Methods). However, the presence of this number of IL-8-stimulated PMN accounted for 1–4% of the measured rate of protein synthesis, and 1–6% of the total production of cytokines, as assessed experimentally in the absence or in the presence of Stx1.

Viability of endothelial cells after transmigration of Stx1-loaded PMN

The viability of HUVEC after transmigration of PMN loaded with different amounts of Stx1 was assessed after overnight incubation by using the vital DNA dye Hoechst 33342 for the detection of changes in chromatin condensation and nuclear morphology and propidium iodide as a probe for membrane

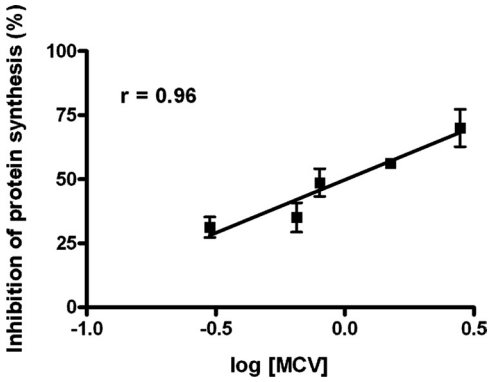

Figure 5. Inhibition of translation in endothelial cells challenged with transmigrating PMN carrying a different amount of Stx1. The binding of Stx1 to PMN was assessed by flow cytometry, as described in Materials and Methods, and expressed as log of MCV. The conditions of Stx binding to PMN from healthy donors and the transmigration assay are described in Materials and Methods. Protein synthesis rate was measured as described in Materials and Methods. The [^{3}H]leucine incorporated by untreated cells was 3404 ± 610 dpm (mean±SD; n=3). Data are means ± SD from three independent experiments. The presence of control transmigrating PMN in the assay did not interfere with endothelial cell translation. The presence of contaminating free Stx coming from the first experimental step (binding of the toxins to PMN) was ruled out by performing appropriate controls in the absence of PMN. r, Correlation coefficient.

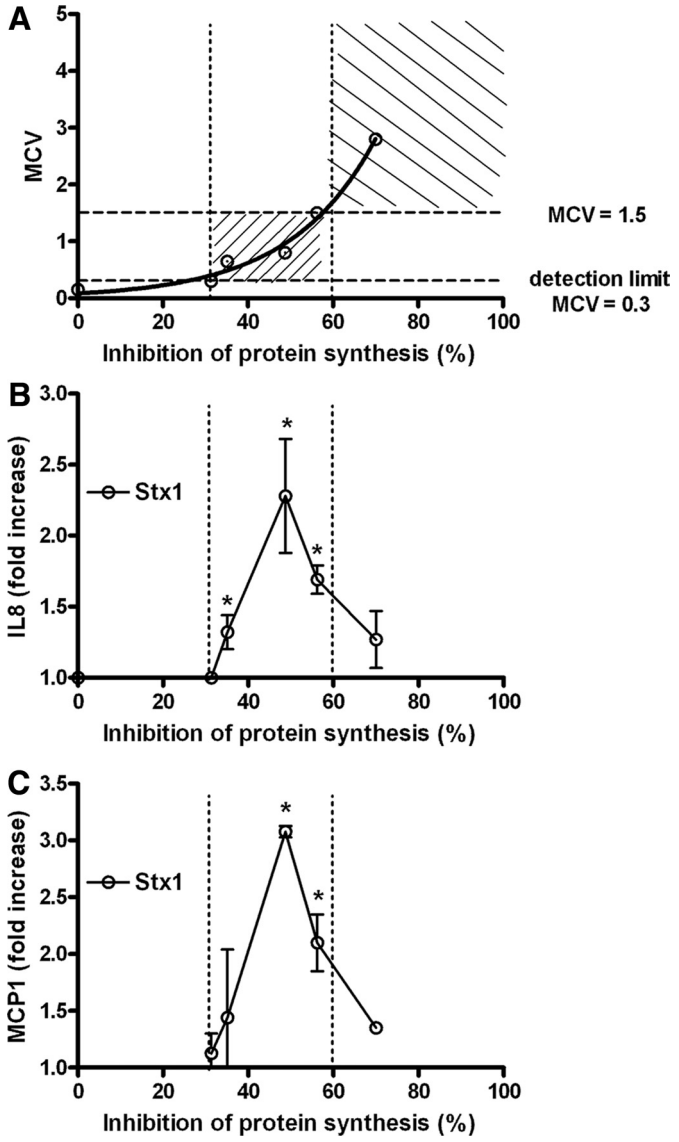

Figure 6. Inhibition of protein synthesis and production of proinflammatory cytokines in HUVEC challenged with Stx1-loaded PMN. (A) Data from Figure 5 about the inhibition of endothelial cell protein synthesis after the transmigration of Stx1-loaded PMN were plotted against the amount of Stx1 present on PMN, detected by flow cytometry, and expressed as MCV. The lower horizontal dotted line represents the detection limit (MCV=0.3) of the flow cytofluorimetric assay described in Materials and Methods to detect Stx bound to PMN. The upper horizontal dotted line indicates the MCV value corresponding to 50% saturation of PMN (MCV=1.5) The two vertical dotted lines indicate the highest (60%) and the lowest (30%) percent of HUVEC protein synthesis inhibition when the endothelial cells were challenged with transmigrating PMN carrying amounts of Stx1 lower than 50% saturation. (B) IL-8 or (C) MCP-1 release by HUVEC treated as described in A. Quantitative determinations of the chemokines present in the culture supernatants were performed by ELISA, as described in Materials and Methods. Data are means ± SD from three or two independent experiments, respectively. The ratios between the amounts of chemokines detected in culture supernatants from toxin-treated cells and those from untreated controls (IL-8, 2521±234 pg/ml, mean±SD, n=3; MCP-1, 23±4 pg/ml, mean±SD, n=2) give the fold increase. *, $P < 0.05$.

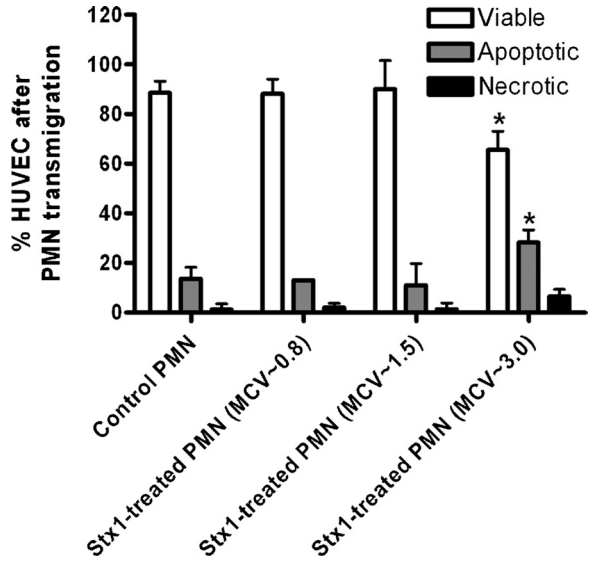

Figure 7. Viability of HUVEC challenged with Stx1-loaded PMN. Detection of apoptosis and necrosis in HUVEC was assessed after transmigration of control PMN and of three populations of PMN carrying different amounts of Stx1 (MCV~0.8; MCV~1.5; MCV~3), which are responsible for the three highest inhibitions of HUVEC translation shown in Figure 6A and of differential up-regulating effects on cytokine production by HUVEC (Fig. 6, B and C). Apoptosis and necrosis were assessed simultaneously by Hoechst 33342 and propidium iodide staining as described in Materials and Methods. Data are means ± SD from three independent experiments. *, $P < 0.05$.

damage. **Figure 7** shows that the percentages of live cells, of cells undergoing apoptosis, and of necrotic cells were unchanged after transmigration of PMN having MCV ≤1.5. Conversely, a significant reduction of live cells accompanied by a significant rise in apoptotic HUVEC was observed after transmigration of fully loaded PMN. This clearly correlated with the strong impairment of protein synthesis measured in these cells (Fig. 6A) and with the concomitant block of cytokine induction (Fig. 6, B and C). Thus, HUVEC challenged with fully loaded PMN developed sudden injuries, which triggered apoptosis in intoxicated cells without producing the proinflammatory cytokines that are secreted when toxic effects on cells are milder.

DISCUSSION

Stx has never been found in the plasma of patients with HUS, and among circulating cells, PMN seem to be the best candidate for the delivery of the toxin from the intestinal mucosa to the renal endothelium. As a matter of fact, PMN account for the greater part of the Stx-binding capacity of blood [17, 23] and possess an affinity for Stx lower than endothelial cells, thus making easier the transfer [17, 22]. However, the interaction between Stx and PMN has been an object of controversy with the presentation of conflicting results. Some authors [18, 19, 38] have reported a lack of specific binding of Stx to PMN, and in particular, Geelen and colleagues [18] interpreted

their own previous results on HUS patients [16, 17] as artifacts as a result of nonspecific binding of anti-Stx antibodies. It should be noted that the first questioned paper [17], never retracted by the corresponding author, reported convincing evidence of Stx binding to PMN, such as immunohistological study and direct flow cytometric analysis with fluorescent toxin, Scatchard plot with iodinated Stx1, and calculation of the dissociation constant and of the number of binding sites on PMN. Moreover, the nonspecific binding of fluorescent anti-Stx antibodies to PMN claimed to justify as an artifact the detection of Stx in patients [16] was simply excluded in the present study by the disappearance of the fluorescent labeling in Stx-positive PMN after transmigration.

In light of the results presented by our group in this study and in previous papers [20, 21, 23] and by Griener et al. [22], the above-mentioned negative results [18, 19, 38] could be explained by some features of their experimental procedures. The studies from Geelen et al. [18] and Flagler et al. [19] reported the lack of binding of Stx1 to neutrophils after treatment with the toxin, followed by the isolation of the cells on Ficoll layers or Mono-Poly resolving media. These treatments could have caused the detachment of Stx from the PMN membrane, as the dissociation constant of the interaction Stx1/neutrophil receptor is fairly elevated with respect to the dissociation constant calculated with the Gb3 receptor, although it is important to note that low-affinity binding does not mean nonspecific binding. Moreover, based on the results presented by Griener et al. [22], indicating that the A subunit of Stx is mainly responsible for the binding to human PMN, it is conceivable that three different active domains may exist in the holotoxin: an enzymic-active site and a Gb3-independent binding site in the A subunit and the well-characterized Gb3-binding sites in the B subunits. It is noteworthy that some of the data obtained in the contrary report by Geelen [18] have been obtained with the B subunit alone, which based on the above findings, could not be involved in PMN binding. Inasmuch, work in progress in our laboratory (manuscript in preparation) demonstrates that depending on the purification procedure, it is possible to obtain Stx preparations lacking PMN-binding activity but maintaining the Gb3-binding and enzymic activities. Thus, the cytotoxicity assays performed in the mentioned negative reports [18, 19, 38], as evidence of the full activity of a given Stx preparation, may not be sufficient to demonstrate the preservation of all of the activities of the toxin. Finally, in studies by Geelen et al. [18] and Flagler et al. [19], a mouse animal model was used. As mouse and human PMN have been shown to possess different Stx-binding receptors [22, 23], the results obtained by this model can hardly be considered representative of the toxic pathways in HUS patients. The results presented in this paper document further that Stx actually binds to human PMN and support the results obtained by analyzing PMN from HUS patients [21].

To understand whether Stx bound to PMN is delivered to endothelial cells, and PMN loaded with different amounts of toxin can elicit different responses in endothelia, we used an experimental model consisting of endotoxin-free PMN [28], migrating through a confluent monolayer of human endothelial cells in a two-chamber transmigration device. To date, the most accredited model centered on the circulating PMN as toxin carriers capable of transferring the toxin to sensitive cells was proposed by te Loo et al. [17] and confirmed recently by Griener [22]. In such a model, coincubation of renal endothelial cells with PMN carrying Stx resulted in the transfer of the toxin to the former cells. This first important evidence, however, was obtained without taking into account the physiological mode of interaction of circulating PMN with endothelia. These interactions occur mainly during leukocyte transmigration in the presence of chemoattractants, whereas they are accidental and scanty in normally flowing blood. Our model included a chemokine-induced transmigration of PMN and a reproducible and quantitative procedure of binding Stx1 to PMN, which allowed us to obtain Stx saturation levels comparable with those observed previously in HUS patients [20, 21]. Stx1 was used in these large-scale experiments, as this toxin was produced in high yield by a simple and rapid purification procedure. Our model still needs to be validated with Stx2, although in previous papers, we did not observe differences between Stx1 and Stx2 in PMN-binding capacity [20, 23]. The results obtained by the model demonstrated that PMN transmigration is not impaired by the presence of Stx1 on their membrane, even at saturating conditions; Stx are transferred from PMN to the endothelial cells during transmigration, as shown by the disappearance of unlabeled or labeled toxins from PMN after transmigration and by the concomitant radioactive labeling of the endothelium. This also indicates that Stx are present on the leukocyte surface, confirming that they are not internalized by PMN [17].

We cannot provide evidence that the transfer mechanism observed in vitro is relevant to the situation in patients with HUS. However, the role of PMN as a Stx carrier in HUS is supported by the following arguments: the presence of the toxic activity of Stx has never been reported in the soluble blood fraction of patients with HUS, although sera from many STEC-infected patients with HUS have been tested by the Vero cells assay [3, 15] and human serum contains neutralizing proteins, such as human serum amyloid P, which prevents the cytotoxicity of Stx2 in vitro but not its binding to human PMN [22, 39].

Our experimental observations also showed that PMN, loaded with different amounts of toxin, induced strikingly different responses in endothelial cells in terms of inflammatory cytokine release. It is well known that internalized Stx cause ribosomal damage, which on one hand induces the inhibition of translation and on the other triggers the stress-kinase cascades that activate transcription of proinflammatory genes in the nucleus [9, 36, 37]. The administration of PMN-bound Stx1 to HUVEC (Fig. 6) showed that IL-8 and MCP-1 production increased progressively with the increase in translation inhibition and then fell down when it was higher than 60%. These differential, up-regulating effects on cytokine production were obtained when Stx1-loaded PMN transmigrated through the HUVEC monolayers: PMN carrying low Stx levels (<50% saturation) caused an inhibition of protein synthesis lower than 60% in endothelial cells, accompanied by a strong up-regulating effect on cytokine production. Conversely, the transmigration of PMN with high Stx levels (full saturation)

caused a block of translation >60% and the activation of the apoptotic program, with the concomitant impairment of IL-8 and MCP-1 induction (Figs. 6 and 7). The involvement of contaminant molecules, such as LPS, in these experiments was excluded by the inhibitory effects of mAb to Stx1 on the release of proinflammatory cytokines. On the other hand, the preparation of Stx used in this study contained low amounts of LPS (Materials and Methods). Also, the effects of molecules released by degranulating PMN can be ruled out, as they were lost during the washings necessary to eliminate free, unbound toxins. Finally, the effect of contaminating PMN trapped underneath HUVEC monolayers on the outcomes of HUVEC protein synthesis and cytokine production was negligible.

It is interesting to note that in baboons, experimentally challenged with i.v. infusion of high and low doses of Stx1 [40], the histopathological changes observed in the kidney were less pronounced in the animals challenged with high concentrations of toxin, which had no evidence of thrombotic microangiopathy in 60% of glomeruli. Conversely, in the low-dose group, only 7% of glomeruli showed no evidence of thrombotic microangiopathy, and 40% and 41% exhibited endothelial swelling and combined endothelial swelling and red corpuscle fragmentation, respectively [40]. Our in vitro results could explain the apparent paradox that the baboons challenged i.v. with high doses of Stx1 [40] had a less pronounced renal involvement. In the presence of high levels of Stx, the production of proinflammatory cytokines is indeed hindered almost completely by the strong inhibition of protein synthesis (Fig. 6) and by the triggering of an apoptotic program in these cells (Fig. 7). Notably, in the baboon model, the production of proinflammatory mediators was localized in the renal tissues [40]. It is therefore conceivable that also in patients with HUS, different levels of toxins in blood may result in different clinical presentations, and renal involvement is inversely related to the amounts of Stx on PMN. Further studies about PMN from HUS patients are needed to evaluate this hypothesis.

The model used to reproduce what might happen in the kidney of HUS patients is limited by the obvious differences with the microenvironment of the fenestrated glomerular endothelia. Anyway, it is possible to speculate about the trigger, which in vivo, might initiate the process of Stx transfer from circulating PMN to endothelia under preinflammatory conditions. The primum movens could be the transfer of a limited number of toxin molecules during the scarce and casual contacts between the PMN and the endothelium. The first toxin molecules transferred would cause subtle ribosomal damage and the consequent secretion of low amounts of IL-8 by the intoxicated cells. The released IL-8, in turn, would stimulate the recruitment and the transmigration of new Stx-positive PMN, thus activating a self-amplifying process, leading to the production of several proinflammatory mediators of renal damage, until endothelial cells undergo to apoptosis. The mechanism proposed is centered on the direct effect of Stx on Gb3-containing endothelia; however, we have shown in this paper that Stx1-saturated PMN are activated and degranulated (Fig. 3). In vivo, the associated release of harmful products might impose further injuries to the surrounding endothelia, depending on the site of degranulation. Moreover, our data about Stx-induced degranulation could explain the observation that PMN from HUS patients show limited response to degranulating stimuli [24, 38], supporting the concept that they have been activated previously and degranulated by Stx (Fig. 4).

In conclusion, our experimental model allowed us to demonstrate that in vitro, Stx bound to PMN are mainly transferred to endothelial cells during the chemokine-induced transmigration of these blood cells. The transmigration of PMN carrying low levels of Stx induced the release of amounts of cytokines much higher than those released by cells challenged with PMN loaded with high levels of toxin. The data obtained by this experimental model could represent a useful background for clinical studies aimed at better defining the role of PMN as a toxin carrier in HUS and investigating the relationship between the amounts of Stx present on the PMN and the clinical presentation of HUS patients.

AUTHORSHIP

M. B., P. L. T., and A. C. conceived and designed the experiments. M. B., E. R., D. C., S. B., L. R., V. A., F. R., and R. R. A. performed the experiments. M. B., P. L. T., E. R., D. C., S. B., L. R., V. A., G. S. F. R., A. B., R. R. A., P. G. P, C. P., A. E. T., and A. C. analyzed and the interpreted data. M. B, A. E. T., and A. C. wrote the paper.

ACKNOWLEDGMENTS

This work was supported by the University of Bologna (RFO funds, M. B.), by the Ministry of Education, University and Research (COFIN 2004, M. B.), and by the Center for Disease Control of the Ministry of Health (A. C.).

DISCLOSURE

The authors declare no competing financial interests.

REFERENCES

1. Trompeter, R. S., Schwartz, R., Chantler, C., Dillon, M. J., Haycock, G. B., Kay, R., Barratt, T. M. (1983) Hemolytic-uremic syndrome: an analysis of prognostic features. *Arch. Dis. Child.* **58,** 101–105.
2. Griffin, P. M., Tauxe, R. V. (1991) The epidemiology of infections caused by *Escherichia coli* O157:H7, other enterohemorrhagic *E. coli*, and the associated hemolytic uremic syndrome. *Epidemiol. Rev.* **13,** 60–98.
3. Karmali, M. A., Petric, M., Lim, C., Fleming, P. C., Arbus, G. S., Lior, H. (1985) The association between idiopathic hemolytic uremic syndrome and infection by verotoxin-producing *Escherichia coli*. *J. Infect. Dis.* **151,** 775–782.
4. Tozzi, A. E., Caprioli, A., Minelli, F., Gianviti, A., De Petris, L., Edefonti, A., Montini, G., Ferretti, A., De Palo, T., Gaido, M., Rizzoni, G. (2003) Shiga toxin-producing *Escherichia coli* infections associated with hemolytic uremic syndrome, Italy, 1988–2000. *Emerg. Infect. Dis.* **9,** 106–108.
5. Noris, M., Remuzzi, G. (2005) Hemolytic uremic syndrome. *J. Am. Soc. Nephrol.* **16,** 1035–1050.
6. Ray, P. E., Liu, X. H. (2001) Pathogenesis of Shiga toxin-induced hemolytic uremic syndrome. *Pediatr. Nephrol.* **16,** 823–839.
7. Paton, J. C., Paton, A. W. (1998) Pathogenesis and diagnosis of Shiga toxin-producing *Escherichia coli* infections. *Clin. Microbiol. Rev.* **11,** 450–479.
8. Endo, Y., Tsurugi, K., Yutsudo, T., Takeda, Y., Ogasawara, T., Igarashi, K. (1988) Site of action of a Vero toxin (VT2) from *Escherichia coli* O157:H7 and of Shiga toxin on eukaryotic ribosomes. RNA N-glycosidase activity of the toxins. *Eur. J. Biochem.* **171,** 45–50.

9. Brigotti, M., Carnicelli, D., Ravanelli, E., Vara, A. G., Martinelli, C., Alfieri, R. R., Petronini, P. G., Sestili, P. (2007) Molecular damage and induction of proinflammatory cytokines in human endothelial cells exposed to Shiga toxin 1, Shiga toxin 2, and {α}-sarcin. *Infect. Immun.* **75,** 2201–2207.
10. Brigotti, M., Alfieri, R., Sestili, P., Bonelli, M., Petronini, P. G., Guidarelli, A., Barbieri, L., Stirpe, F., Sperti, S. (2002) Damage to nuclear DNA induced by Shiga toxin 1 and ricin in human endothelial cells. *FASEB J.* **16,** 365–372.
11. Nakao, H., Takeda, T. (2000) *Escherichia coli* Shiga toxin. *J. Nat. Toxins* **9,** 299–313.
12. Sestili, P., Alfieri, R., Carnicelli, D., Martinelli, C., Barbieri, L., Stirpe, F., Bonelli, M., Petronini, P. G., Brigotti, M. (2005) Shiga toxin 1 and ricin inhibit the repair of H2O2-induced DNA single strand breaks in cultured mammalian cells. *DNA Repair (Amst.)* **4,** 271–277.
13. Matussek, A., Lauber, J., Bergau, A., Hansen, W., Rohde, M., Dittmar, K. E., Gunzer, M., Mengel, M., Gatzlaff, P., Hartmann, M., Buer, J., Gunzer, F. (2003) Molecular and functional analysis of Shiga toxin-induced response patterns in human vascular endothelial cells. *Blood* **102,** 1323–1332.
14. Zoja, C., Angioletti, S., Donadelli, R., Zanchi, C., Tomasoni, S., Binda, E., Imberti, B., te Loo, M., Monnens, L., Remuzzi, G., Morigi, M. (2002) Shiga toxin-2 triggers endothelial leukocyte adhesion and transmigration via NF-κB dependent up-regulation of IL-8 and MCP-1. *Kidney Int.* **62,** 846–856.
15. Caprioli, A., Luzzi, I., Rosmini, F., Pasquini, P., Cirrincione, R., Gianviti, A., Matteucci, M. C., Rizzoni, G. (1992) Hemolytic-uremic syndrome and Vero cytotoxin-producing *Escherichia coli* infection in Italy. The HUS Italian Study Group. *J. Infect. Dis.* **166,** 154–158.
16. Te Loo, D. M., van Hinsbergh, V. W., van den Heuvel, L. P., Monnens, L. A. (2001) Detection of verocytotoxin bound to circulating polymorphonuclear leukocytes of patients with hemolytic uremic syndrome. *J. Am. Soc. Nephrol.* **12,** 800–806.
17. Te Loo, D. M., Monnens, L. A., van Der Velden, T. J., Vermeer, M. A., Preyers, F., Demacker, P. N., van Den Heuvel, L. P., van Hinsbergh, V. W. (2000) Binding and transfer of verocytotoxin by polymorphonuclear leukocytes in hemolytic uremic syndrome. *Blood* **95,** 3396–3402.
18. Geelen, J. M., van der Velden, T. J., Te Loo, D. M., Boerman, O. C., van den Heuvel, L. P., Monnens, L. A. (2007) Lack of specific binding of Shiga-like toxin (verocytotoxin) and non-specific interaction of Shiga-like toxin 2 antibody with human polymorphonuclear leukocytes. *Nephrol. Dial. Transplant.* **22,** 749–755.
19. Flagler, M. J., Strasser, J. E., Chalk, C. L., Weiss, A. A. (2007) Comparative analysis of the abilities of Shiga toxins 1 and 2 to bind to and influence neutrophil apoptosis. *Infect. Immun.* **75,** 760–765.
20. Tazzari, P. L., Ricci, F., Carnicelli, D., Caprioli, A., Tozzi, A. E., Rizzoni, G., Conte, R., Brigotti, M. (2004) Flow cytometry detection of Shiga toxins in the blood from children with hemolytic uremic syndrome. *Cytometry B Clin. Cytom.* **61,** 40–44.
21. Brigotti, M., Caprioli, A., Tozzi, A. E., Tazzari, P. L., Ricci, F., Conte, R., Carnicelli, D., Procaccino, M. A., Minelli, F., Ferretti, A. V., Paglialonga, F., Edefonti, A., Rizzoni, G. (2006) Shiga toxins present in the gut and in the polymorphonuclear leukocytes circulating in the blood of children with hemolytic-uremic syndrome. *J. Clin. Microbiol.* **44,** 313–317.
22. Griener, T. P., Mulvey, G. L., Marcato, P., Armstrong, G. D. (2007) Differential binding of Shiga toxin 2 to human and murine neutrophils. *J. Med. Microbiol.* **56,** 1423–1430.
23. Brigotti, M., Carnicelli, D., Ravanelli, E., Barbieri, S., Ricci, F., Bontadini, A., Tozzi, A. E., Scavia, G., Caprioli, A., Tazzari, P. L. (2008) Interactions between Shiga toxins and human polymorphonuclear leukocytes. *J. Leukoc. Biol.* **84,** 1019–1027.
24. Fernandez, G. C., Gomez, S. A., Ramos, M. V., Bentancor, L. V., Fernandez-Brando, R. J., Landoni, V. I., Lopez, L., Ramirez, F., Diaz, M., Alduncin, M., Grimoldi, I., Exeni, R., Isturiz, M. A., Palermo, M. S. (2007) The functional state of neutrophils correlates with the severity of renal dysfunction in children with hemolytic uremic syndrome. *Pediatr. Res.* **61,** 123–128.
25. Ryd, M., Alfredsson, H., Blomberg, L., Andersson, A., Lindberg, A. A. (1989) Purification of Shiga toxin by α-D-galactose-(1-4)-β-D-galactose-(1-4)-β-D-glucose-(1–) receptor ligand-based chromatography. *FEBS Lett.* **258,** 320–322.
26. Maier, J. A., Voulalas, P., Roeder, D., Maciag, T. (1990) Extension of the life-span of human endothelial cells by an interleukin-1 α antisense oligomer. *Science* **249,** 1570–1574.
27. Petronini, P. G., Tramacere, M., Mazzini, A., Piedimonte, G., Silvotti, L., Borghetti, A. F. (1987) Hyperosmolarity-induced stress proteins in chick embryo fibroblasts. *Exp. Cell Res.* **172,** 450–462.
28. Cassatella, M. A., Cappelli, R., Della Bianca, V., Grzeskowiak, M., Dusi, S., Berton, G. (1988) Interferon-γ activates human neutrophil oxygen metabolism and exocytosis. *Immunology* **63,** 499–506.
29. Van Setten, P. A., Monnens, L. A., Verstraten, R. G., van den Heuvel, L. P., van Hinsbergh, V. W. (1996) Effects of verocytotoxin-1 on nonadherent human monocytes: binding characteristics, protein synthesis, and induction of cytokine release. *Blood* **88,** 174–183.
30. Bradford, M. M. (1976) A rapid and sensitive method for the quantitation of microgram quantities of protein utilizing the principle of protein-dye binding. *Anal. Biochem.* **72,** 248–254.
31. Borregaard, N., Sorensen, O. E., Theilgaard-Monch, K. (2007) Neutrophil granules: a library of innate immunity proteins. *Trends Immunol.* **28,** 340–345.
32. Soehnlein, O., Weber, C., Lindbom, L. (2009) Neutrophil granule proteins tune monocytic cell function. *Trends Immunol.* **30,** 538–546.
33. Soehnlein, O., Zernecke, A., Weber, C. (2009) Neutrophils launch monocyte extravasation by release of granule proteins. *Thromb. Haemost.* **102,** 198–205.
34. Brigotti, M., Carnicelli, D., Ravanelli, E., Vara, A. G., Martinelli, C., Alfieri, R. R., Petronini, P. G., Sestili, P. (2007) Molecular damage and induction of proinflammatory cytokines in human endothelial cells exposed to Shiga toxin 1, Shiga toxin 2, and α-sarcin. *Infect. Immun.* **75,** 2201–2207.
35. Morigi, M., Galbusera, M., Binda, E., Imberti, B., Gastoldi, S., Remuzzi, A., Zoja, C., Remuzzi, G. (2001) Verotoxin-1-induced up-regulation of adhesive molecules renders microvascular endothelial cells thrombogenic at high shear stress. *Blood* **98,** 1828–1835.
36. Iordanov, M. S., Pribnow, D., Magun, J. L., Dinh, T. H., Pearson, J. A., Chen, S. L., Magun, B. E. (1997) Ribotoxic stress response: activation of the stress-activated protein kinase JNK1 by inhibitors of the peptidyl transferase reaction and by sequence-specific RNA damage to the α-sarcin/ricin loop in the 28S rRNA. *Mol. Cell. Biol.* **17,** 3373–3381.
37. Smith, W. E., Kane, A. V., Campbell, S. T., Acheson, D. W., Cochran, B. H., Thorpe, C. M. (2003) Shiga toxin 1 triggers a ribotoxic stress response leading to p38 and JNK activation and induction of apoptosis in intestinal epithelial cells. *Infect. Immun.* **71,** 1497–1504.
38. Fernandez, G. C., Gomez, S. A., Rubel, C. J., Bentancor, L. V., Barrionuevo, P., Alduncin, M., Grimoldi, I., Exeni, R., Isturiz, M. A., Palermo, M. S. (2005) Impaired neutrophils in children with the typical form of hemolytic uremic syndrome. *Pediatr. Nephrol.* **20,** 1306–1314.
39. Marcato, P., Vander Helm, K., Mulvey, G. L., Armstrong, G. D. (2003) Serum amyloid P component binding to Shiga toxin 2 requires both a subunit and B pentamer. *Infect. Immun.* **71,** 6075–6078.
40. Taylor Jr., F. B., Tesh, V. L., DeBault, L., Li, A., Chang, A. C., Kosanke, S. D., Pysher, T. J., Siegler, R. L. (1999) Characterization of the baboon responses to Shiga-like toxin: descriptive study of a new primate model of toxic responses to Stx-1. *Am. J. Pathol.* **154,** 1285–1299.

KEYWORDS:
hemolytic uremic syndrome · polymorphonuclear leukocytes · endothelial cells · proinflammatory cytokine · degranulation